

Study of operating modes of electromagnetic hammer with adjustable impact energy and blow frequency

Ayman Y. Al-Rawashdeh¹, Vlademer E. Pavlov²

¹Department of Electrical Engineering, Faculty of Engineering Technology, Al-Balqa Applied University, Amman, Jordan

²Department of Mechatronics Engineering, Irkutsk National Research Technical University, Irkutsk, Russia

Article Info

Article history:

Received Jan 25, 2023

Revised Jun 30, 2023

Accepted Jul 20, 2023

Keywords:

Electromagnetic hammer

Idle stroke winding

Position sensors

Striker

Working stroke winding

ABSTRACT

The current work was designed to study the operating modes of electromagnetic impact mechanism (electromagnetic hammer) comprising idle and working stroke windings that are enclosed in magnetic conductor, and reciprocating ferromagnetic striker. Investigation was conducted by modelling in MATLAB environment and performing verification tests with different hammers. Simulation model of the hammer was derived using experimentally obtained static characteristic curves of flux linkage and thrust force for each of the windings. Results revealed that at maximum working stroke winding voltage-varying idle stroke winding voltage, the impact energy did not change, but the impact frequency varied between 0-187 bpm. At maximum idle stroke winding voltage and working stroke winding voltage ranging between 0 to maximum value, the impact energy varied between 84-360 J, the impact frequency varied between 96-187 bpm. Maximum losses over the working cycle were associated with electric losses in the hammer windings and can be reduced by reducing winding currents through increasing the striker speed. The mathematical model of the current study allowed quantifying energy parameters of the electromagnetic hammer. The impact machine cycle includes three operating modes, each determines the main energy parameters: efficiency, impact energy, and cycle time.

This is an open access article under the [CC BY-SA](https://creativecommons.org/licenses/by-sa/4.0/) license.



Corresponding Author:

Ayman Y. Al-Rawashdeh

Department of Electrical Engineering, Faculty of Engineering Technology, Al-Balqa Applied University

Amman, 11134, Jordan

Email: dr.ayman.rawashdeh@bau.edu.jo

1. INTRODUCTION

Experience gained during operation of electric machines (i.e., those using electromagnetic forces) in different industry sectors allows identifying the most promising areas of their further application. Many researchers [1]–[5] are currently studying issues related to effective use of linear electromagnetic drives in various production processes. Electromagnetic impact machines (electromagnetic hammers) are used for breaking rocks, driving piles, developing frozen soils, in offshore oilfield construction, and as well-bore vibration sources [6], [7].

One of the most crucial tasks in the development of such hammers is improvement of energy performance per cycle. Energy conversion issues in electromagnetic impact machines are among the most complex ones [8]–[13]. Energy conversion efficiency is intimately connected with formation of the operational cycle of electromagnetic machines. Previous research work in this field reported many important recommendations as to the formation of the operational cycle of electromagnetic machines [14]–[18].

Implementation of those recommendations helped in achieving either maximum speed performance or the best efficiency of the machine.

Determination of the required single impact energy is an essential condition to be considered in the design of impact machines. This is due to the fact that rock fracturing does not assume constant correspondence between the material strength and drive loading, which is typical for static machines, such as machines that use cutting tools. If a static machine is fitted with an overpowered motor, the motor will still consume only the power conditioned by a given load (strength of specific rock and actual dulling of the cutting tool). The same behavior is not true in case of impact machines. Even if the single impact energy appears to be excessive for fracturing of a certain rock, all the energy stored by the striker will be consumed.

The excess work will either be absorbed by the oversized material or will be used for over crushing of the treated material. Therefore, selection of the correct single impact energy is essential. Quantitative assessment of specific energy consumption for crushing of oversized rocks was studied in a large number of researches [19]–[21]. Operating cycle of electromagnetic hammer consists of the following stages:

- Build-up of current in the idle stroke winding up to the starting current;
- Upward striker movement until stop (idle stroke); and
- Downward striker movement until delivering a blow (working stroke).

The striker accumulates potential energy during its upward motion (idle stroke mode). This energy is converted into kinetic energy during the working stroke. Potential energy is proportional to the striker rising height (stroke), while cyclic time of the hammer (i.e., the impact frequency) depends on the movement time. Therefore, the striker travel is a controlled parameter, which determines the main performance characteristics of the hammer.

Deceleration and stoppage of the striker during its idle stroke may occur under the effect of braking forces acting opposite to the direction of motion (weight of the striker and friction forces), as well as due to the forces created by braking devices (mechanical springs, and air bumpers). At that point, the striker slows down, and kinetic energy accumulated by the striker is converted into potential energy, and can be partially used during the working stroke of the striker. The starting moment of the deceleration mode and its intensity defines the travel of the striker and the deceleration time and, therefore, the impact frequency and impact energy.

As the striker moves downward (working stroke mode), potential energy accumulated during the idle stroke is converted into kinetic energy. Besides, downward striker speed can be further increased due to the traction force created by the working stroke winding. Electromechanical systems with electromagnetic hammer were designed and built taking into account particular issues associated with the conversion of energy during machine operation and the required ability to control main energy parameters of the electromagnetic drive. The current study aims at obtaining quantitative estimation of energy parameters of electromagnetic hammer per operating cycle through a mathematical model of the machine.

2. THEORITICAL BACKGROUND

Analytical methods for calculating the dynamic behavior of electromagnetic machines are based on the magnetic circuit theory. During the calculations, a magnetic system is replaced by an equivalent electrical circuit. At this stage, the calculation of the electromagnet thrust force requires accurate accounting of the leakage flux distribution, which is considered to be quite difficult when using the existing approaches [22], [23]. The research findings presented in this work were obtained using computer modelling in MATLAB-based Simulink simulation environment. The initial differential equation system for each of the electromagnets is as follows:

$$\begin{aligned} U &= R i \frac{d\psi(i, \delta)}{dt}, \\ m \frac{dV}{dt} &= Fe(i, \delta) - Fc(\delta, V), \\ m \frac{d\delta}{dt} &= V \end{aligned} \quad (1)$$

where: U : the applied voltage; R : active resistance of the winding; i : instantaneous winding current; ψ : flux linkage; δ : the air gap; m : mass; V : speed of the striker; Fe : the electromagnet traction force; and Fc : the resistive force to motion of the striker.

3. PROPOSED METHOD

As shown in Figure 1, the hammer consists of dummy (LM1) and working (LM2) coils enclosed in a magnetic tube, and a ferromagnetic striker, which performs reciprocating motion. The coils are powered by

controlled rectifiers V1 and V2, that operate according to the commands from the control unit B. This unit receives the signals of set points U_{m1} and U_{m2} , as well as signals from the sensors of the lower S1 and upper S2 positions of the striker, on the basis of which the unit controls the working cycle of the hammer.

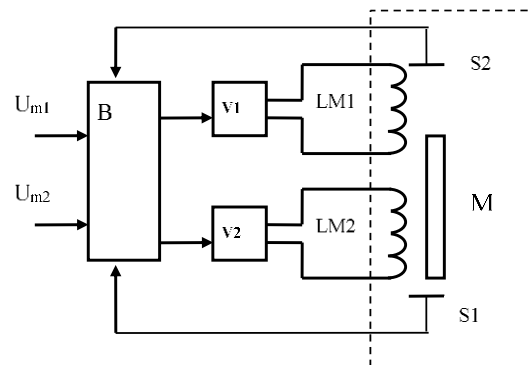


Figure 1. Electromagnetic hammer

The hammer coils are alternately supplied with direct current from controlled inverters. The model contains two such converters, controlled by the control unit B, which inputs the signals from the striker position sensors. The following parameters are calculated in the model: the current position of the striker, the values of the coil linkages and currents, as well as the coil traction forces with regard to the traction characteristics of the hammer changing in the process of movement. The model uses experimentally taken static characteristics of the flux-circuitry and traction force of this hammer as shown in Figures 2(a) and 2(b).

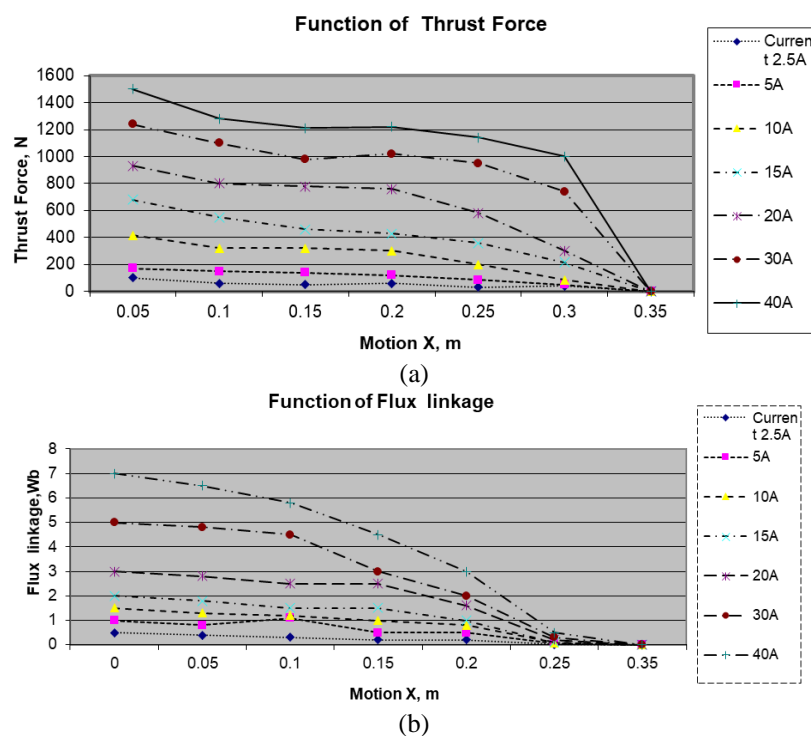


Figure 2. Effect of series resistances on the (a) I-V and (b) P-V characteristics

Dynamic behavior of electromagnetic machines can be quite accurately studied using mathematical models, which take into account the main nonlinearities in dynamic characteristics of its individual

components. Computer simulation modelling using MATLAB-based Simulink environment is currently used to study behavior of objects in systems of virtually unlimited complexity. An important advantage of this method is the ability to monitor the process over time.

The hammer model as shown in Figure 3 is designed according to the function block diagram of the hammer itself (Figure 1) and the system of (1) used for each of the machine coils. The parameters of the dummy coils and the value of current, flux linkage, and traction force created by this coil are indicated in the model with index 1. The same parameters and values created by the working coil are indicated in the model with index 2. The coils operate in turn, according to signals from the input device (U_{m1} , U_{m2}) and from striker position sensors (S1, S2). Initially, the striker is in the lower position (Figure 1), it is completely placed in the coil of the lower second electromagnet and partially enters the coil of the upper first electromagnet. To start the hammer and its model, the $Rect_1$ rectifier mode is turned on and voltage is supplied to the dummy coil, a current i_1 appears, the value of which depends on the active and inductive resistance of the coil (block B1).

The current i_1 creates the traction force of the coil F_1 . The magnitude of this force depends on the striker position inside the dummy coil. If the force F_1 is greater than the movement resistance forces F_c applied on the adder in the model, then the striker will start moving upwards. The speed of movement and position of the striker are determined in the model using integration blocks. When moving the striker, the values of flux linkage, inductance, current and traction force of the electromagnet change. These changes are taken into account and calculated in the model using blocks B3 and B4. When the striker reaches the upper position sensor S1, a signal is transferred to the control unit B, converting the rectifier that feeds the dummy winding to the inverter mode. The signal $Rect_1$ disappears in the model and signal $Inv1$ appears. The current i_1 is reduced to zero and the field of the upper electromagnet is damped. The striker starts moving down. At the same time, according to the signal from the sensor S1, the $Rect_2$ rectifier mode is turned on and the voltage is supplied to the working coil, the current i_2 appears, the value of which depends on the active and inductive resistance of the coil (block B2). The current i_2 creates the traction force of the coil F_2 . The magnitude of this force depends on the position of the striker inside the working coil. The striker accelerates due to the appearance of the F_2 force. When moving the striker, the values of flux linkage, inductance, current and traction force of the electromagnet change. These changes are taken into account and calculated in the model using blocks B5 and B6. When the striker reaches the lower position sensor S2, a signal is transferred to the control unit B, converting the rectifier that feeds the dummy winding to the inverter mode. The $Rect_2$ signal disappears in the model and signal Inv_2 appears. The current i_2 is reduced to zero and the field of the lower electromagnet is damped. The hammer strikes. At the same time, according to the signal from sensor S2, the $Rect_1$ rectifier mode is turned on and voltage is supplied to the dummy coil, current i_1 appears. The cycle of operation of the hammer model is repeated.

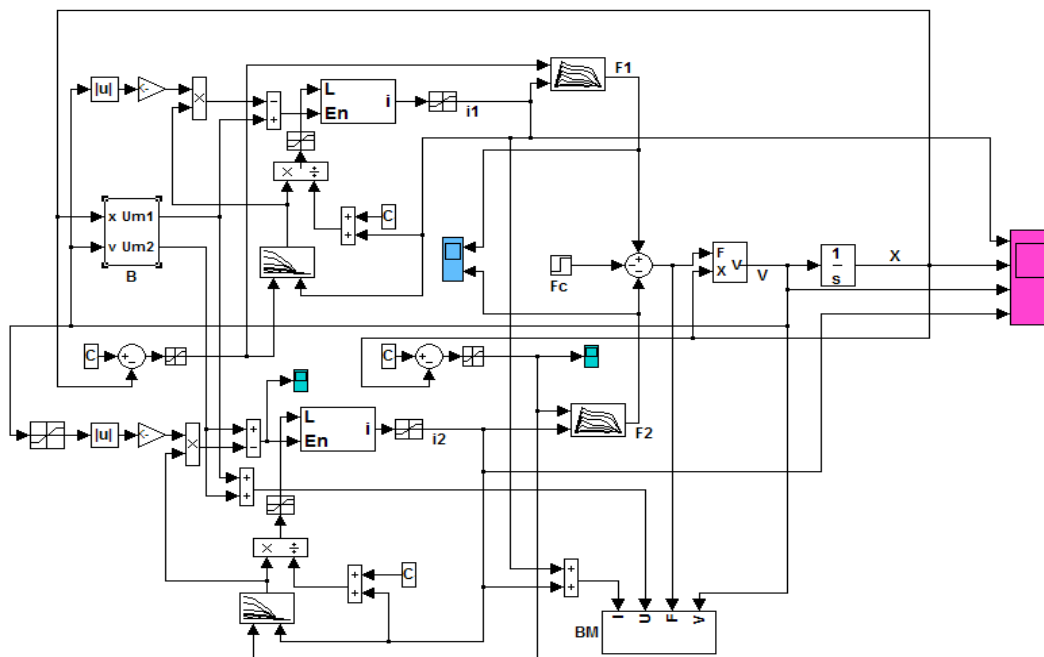


Figure 3. Electromagnetic hammer model

For illustrative purposes, let us consider electromagnetic hammer having striker with a mass of 22 kg, and an active resistance (obtained by experimental measurements) shown in Figure 3. Mathematical model of the hammer, which was developed based on the equations of system (1) and using static characteristics for each of the windings obtained by measurement, is shown in Figure 4. The model contains the control block B Figure 4(a), two current calculation blocks B1 and B2 Figure 4(b), two blocks for calculation of the flux linkage, two blocks for calculation of the winding thrust force, as well as measurement block BM.

Theoretical studies have been carried out using the methods of field theory and mathematical apparatus of linear and nonlinear differential equation systems. The calculations have been carried out on models using MATLAB. Experimental studies have been carried out with simulation methods and full-scale tests on various hammers.

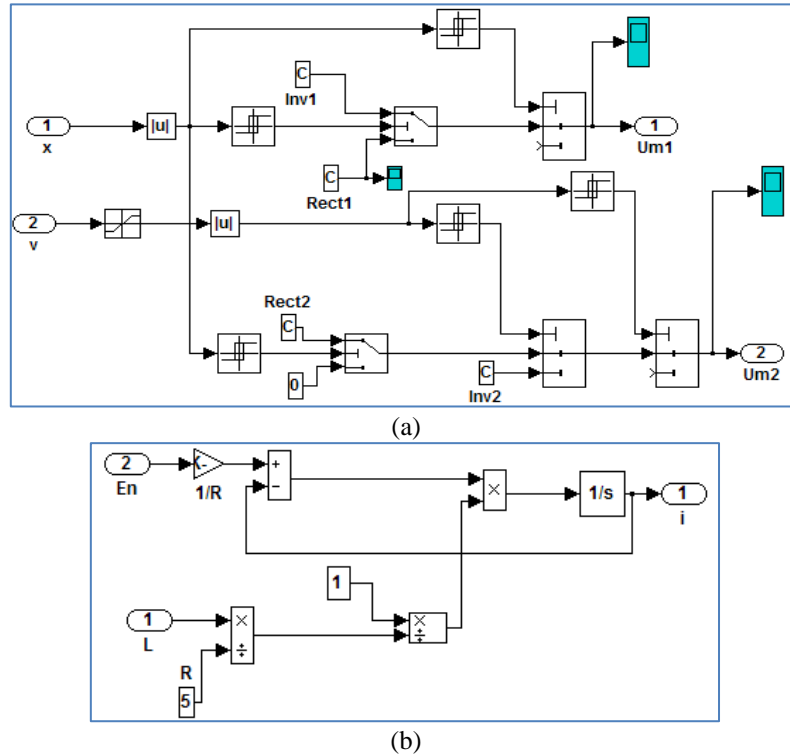


Figure 4. Electromagnetic hammer model: (a) model of the control block B and (b) model of the current calculation blocks B1 and B2

The control block, which forms operation cycle of the hammer, contains four voltage sources for rectifying ($Rect_1$, $Rect_2$) and inverter (Inv_1 , Inv_2) modes of the idle stroke and working stroke winding power supplies; relay and threshold elements that ensure connection of these power sources to the corresponding winding by signals from the striker travel and linear speed sensors.

Current calculation blocks Figure 4(b) B1 and B2 determine the instantaneous winding currents by the formula:

$$i = [U - kV\Psi(i; \delta)] \frac{1/R}{Tp+1},$$

where k is the hammer design factor; p is the p -Laplace operator; T is the electromagnetic time constant of the hammer winding.

$$T = \frac{L(i; \delta)}{R}$$

where $L(i, \delta)$ is inductance of the hammer winding, defined as:

$$L(i; \delta) = \frac{\Psi(i; \delta)}{i}$$

BM measurement block allows determining instantaneous mains power consumption $P_1 = U_i$; copper losses in the hammer windings $P_m = i_2 R$; mechanical power $P_{\text{mech}} = F_2 V$. Mains power consumption W_1 , copper losses in the hammer windings W_m , mechanical power of the hammer W_{mech} are obtained by integrating the corresponding power values.

The proposed analytical methods for calculating such systems, when deriving the main calculation expressions, abound in many assumptions and limitations concerning the consideration of magnetic resistances and parasitic gaps, dissipation and convex fluxes, and the range of variation of the operating gap [24]. Most importantly, the results of calculations using known expressions and experimental data for newly created devices in practice can have large discrepancies. This is primarily because the existing methods for calculating electromagnetic systems are based on the theory of magnetic circuits. In the calculations, the magnetic system is replaced by an electrical substitution diagram, and the values of magnetic resistances are determined from a simplified field picture. The working air gap, where the energy conversion process takes place, also appears to be one of the sections of the magnetic circuit, the resistance of which depends on the dimensions and surfaces of the striker and stationary magnetic core arrangement with some formal consideration of the magnetic flux distribution. In fact, the calculation of the thrust force in long stroke systems is associated with the exact consideration of the distribution of the dissipation fluxes, which causes great difficulties when using the existing approaches. Consequently, there is no simple and sufficiently accurate analytical method for calculating long stroke plunger systems.

The dedicated mathematical program for calculating the two-dimensional magnetic field FEMM is based on the finite element method [25]. There are three main functional units in FEMM: the unit for creating the geometry of the computational domain, identifying and assigning physical properties to its individual parts (preprocessor); the unit for calculating model parameters by the finite element method (processor); the unit for displaying the results of the calculation (postprocessor). The method of computer modeling proposed in our article using the MATLAB-based Simulink simulation environment is currently used to study objects in systems of almost any complexity. The important advantages of this method include the possibility to observe the process in time.

4. RESULTS AND DISCUSSION

Transient processes in terms of coil current, striker speed and stroke, energy consumed from the grid, power losses in copper and impact energy, as well as efficiency have been obtained for the hammer operation cycle. Studies have shown that with the maximum voltage of the working coil and a change in the voltage of the dummy coil, the impact energy does not change, and the frequency of impacts varies from 0 to 187 strokes per minute. With the maximum voltage of the dummy coils and an increase in the voltage of the working coil in the range from 0 to the maximum value, the impact energy increases by 4.3 times, and the frequency of impacts decreases by 1.96 times. The largest value for the operation cycle is the electrical losses in the hammer coils, to reduce them, it is necessary to reduce the magnitude of the coil currents, and to do this it is required to increase the striker speed.

Figure 5 shows Oscillograms of the upper winding current i_1 , linear speed V and stroke X of the striker at voltages $U_1 = 210$ V and $U_2 = 0$ V (as shown in Figure 5(a)); and oscillograms of the upper winding current, linear speed V and stroke X of the striker, lower winding current i_2 at voltages $U_1 = 210$ V and $U_2 = 210$ V (Figure 5(b)). Figure 5(a) shows oscillograms of the upper winding current, linear speed V and stroke X of the striker, obtained from the model, when only the upper winding ($U_1 = 210$ V and $U_2 = 0$ V) is used. Figure 5(b) shows oscillograms of the upper winding current, linear speed V and stroke X of the striker, as well as the lower winding current at voltages $U_1 = 210$ V and $U_2 = 210$ V.

Analysis of the obtained oscillograms allowed the determination the following:

- When only the upper winding is used ($U_2 = 0$ V), time from the zero-point moment to the moment when the striker starts moving is 0.03 s, current at the striker starting moment is 28 A, and the total time of upward travel is 0.33 s
- At voltages $U_1 = 210$ V and $U_2 = 210$ V, time from the zero-point moment to the moment when the striker starts moving is 0.03 s, current at the striker starting moment is 28 A, and the total time of upward travel is 0.21 s
- When only the upper winding is used ($U_2 = 0$ V), the total time of downward striker travel is 0.29 s
- At voltages $U_1 = 210$ V and $U_2 = 210$ V, the total time of downward striker travel is 0.11 s
- When only the upper winding is used ($U_1 = 210$ V and $U_2 = 0$ V), the hammer cycle time makes 0.62 s, number of blows per minute (frequency) $n = 96$ bpm
- At voltages $U_1 = 210$ V and $U_2 = 210$ V, the hammer cycle time makes 0.32 s, number of blows per minute (frequency) $n = 187$ bpm.

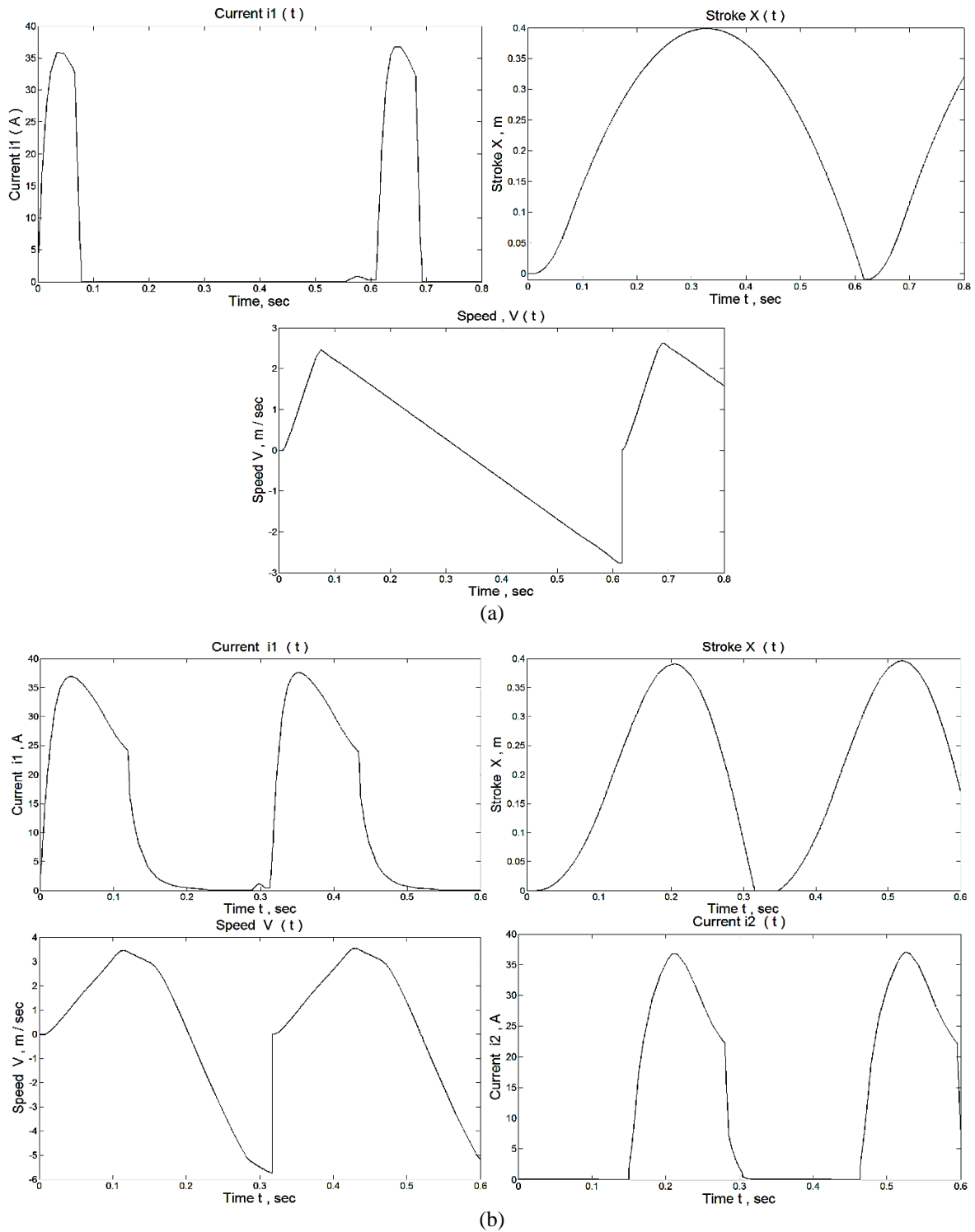


Figure 5. Oscillograms of the upper winding current i_1 , linear speed V and stroke X of the striker at voltages $U_1 = 210 \text{ V}$ and (a) $U_2 = 0 \text{ V}$ in and (b) lower winding current i_2 at voltages $U_1 = 210 \text{ V}$ and $U_2 = 210 \text{ V}$

Analysis of oscillograms shown in Figure 6 allowed the determination of the following:

- When only the idle stroke winding is used ($U_2 = 0 \text{ V}$), copper losses per operation cycle of the hammer make 280 J;
- At voltages $U_1 = 210 \text{ V}$ and $U_2 = 210 \text{ V}$, copper losses per operation cycle of the hammer make 900 J;
- When only the idle stroke winding is used ($U_2 = 0 \text{ V}$), the hammer impact energy makes 84 J;
- At voltages $U_1 = 210 \text{ V}$ and $U_2 = 210 \text{ V}$, the hammer impact energy makes 330 J;

- When only the idle stroke winding is used ($U_2 = 0$ V), power consumed from the mains per operation cycle of the hammer makes 450 J;
- At voltages $U_1 = 210$ V and $U_2 = 210$ V, energy consumed from the mains per operation cycle of the hammer makes 1600 J;
- When only the idle stroke winding is used ($U_2 = 0$ V), efficiency of the hammer per its operation cycle is 14%; and
- At voltages $U_1 = 210$ V and $U_2 = 210$ V, efficiency of the hammer per its operation cycle is 22 %.

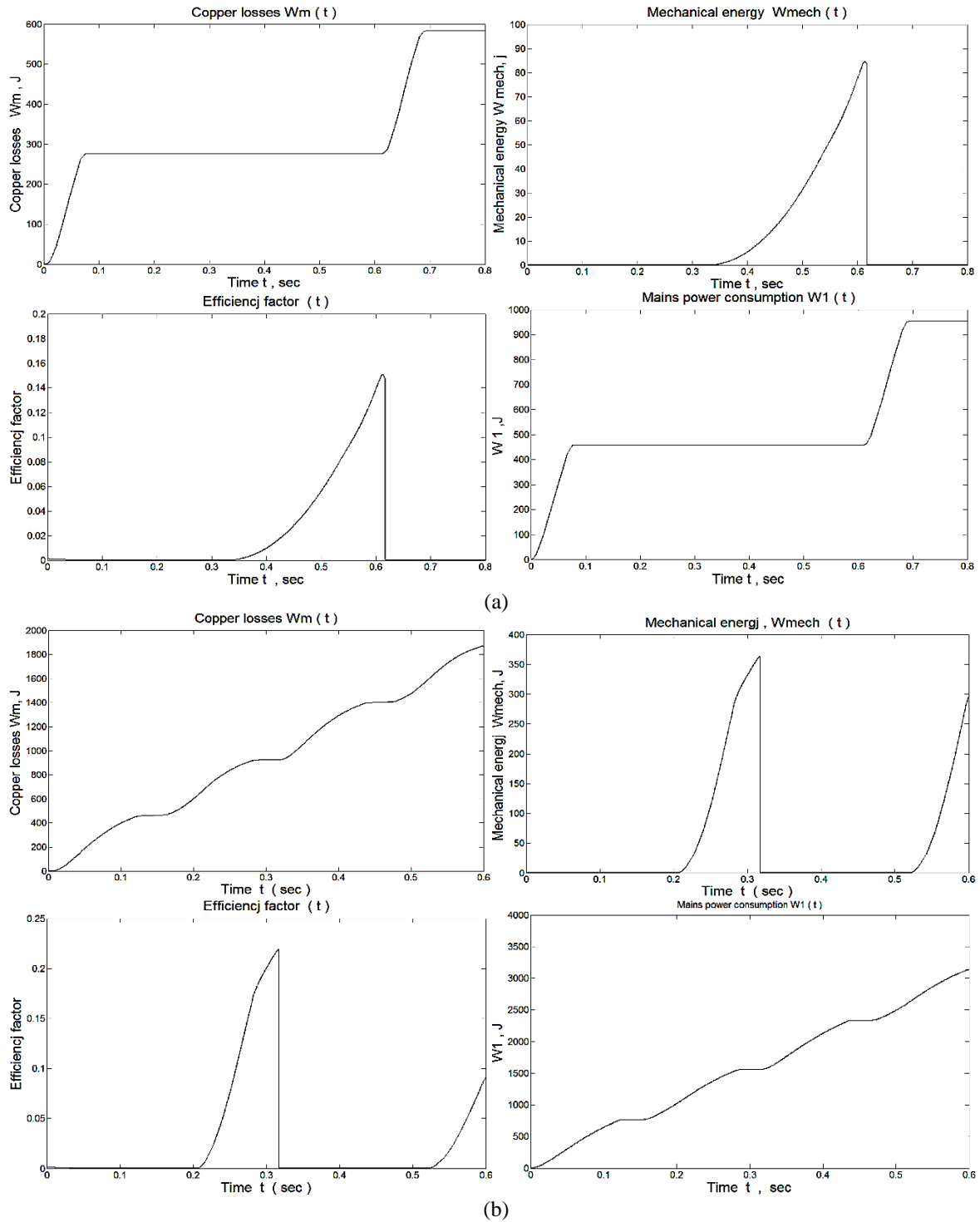


Figure 6. Oscillograms of copper losses W_m , mechanical energy W_{mech} , efficiency η , mains power consumption W_1 over one operation cycle of the hammer at voltages $U_1 = 210$ V, (a) $U_2 = 0$ V and (b) $U_2 = 210$ V

5. CONCLUSION

Mathematical model of the hammer has been developed using the measured static characteristics of flux linkage and traction force for each of the windings. Oscillograms of the idle winding current, working winding current, striker speed and stroke were obtained. Figures for the power consumed from the mains, copper losses and impact energy, as well as the hammer efficiency per operation cycle were determined.

The study has shown that at working stroke winding voltage $U_2 = 210$ V and varying idle stroke winding voltage, the impact energy does not change, while the impact frequency varies between 0 and 187 blows per minute. At idle stroke winding voltage $U_1 = 210$ V and working stroke winding voltage varying in the range from 0 to 210 V, the impact energy varies between 84 and 360 J, and the impact frequency varies between 96 and 187 blows per minute. Maximum losses over the working cycle are associated with electric losses in the hammer windings; those losses may be reduced by reducing winding currents, which in turn requires an increase in the striker speed.

To obtain the maximum machine efficiency in the idle phase, the striker shall be braked by coasting to stop, as such braking does not require consumption of energy by the machine, and the kinetic energy will be completely (excluding losses) converted into potential energy. As can be seen from the above, impact machine cycle includes three operating modes, each of which determines the main energy parameters of the machine: efficiency, impact energy and cycle time. At that, impact energy and frequency of blows of the machine should be selected in accordance with the requirements of the associated process.




REFERENCES

- [1] Y. Sun and Y. Lan, "Optimal design of electromagnetic force of hidden - Pole magnetic suspension linear motor," *IEEE Access*, vol. 7, pp. 153675–153682, 2019, doi: 10.1109/ACCESS.2019.2949002.
- [2] A. Keshkar, Z. Jafari Khorrami, and L. Gharib, "Comparison of Inductance Gradient and Electromagnetic Force in Two Types of Railguns with Two Projectiles by Finite-Element Method," *IEEE Transactions on Plasma Science*, vol. 45, no. 8, pp. 2387–2392, 2017, doi: 10.1109/TPS.2017.2716357.
- [3] C. Xiang, S. A. Chen, M. Yao, Y. F. Gu, and X. Yang, "Optimization of Braking Force for Electromagnetic Track Brake Using Uniform Design," *IEEE Access*, vol. 8, pp. 146065–146074, 2020, doi: 10.1109/ACCESS.2020.3014122.
- [4] L. Qiu *et al.*, "Parametric Simulation Analysis of the Electromagnetic Force Distribution and Formability of Tube Electromagnetic Bulging Based on Auxiliary Coil," *IEEE Access*, vol. 8, pp. 159979–159989, 2020, doi: 10.1109/ACCESS.2020.3020830.
- [5] L. Qiu *et al.*, "Analysis of Electromagnetic Force and Deformation Behavior in Electromagnetic Tube Expansion With Concave Coil Based on Finite Element Method," *IEEE Transactions on Applied Superconductivity*, vol. 28, no. 3, 2018, doi: 10.1109/TASC.2017.2789287.
- [6] V. Y. Neyman, V. M. Less, and A. V. Prokopov, "Linear electromagnetic motor with periodic structure of magnetic circuit," *IOP Conference Series: Materials Science and Engineering*, vol. 560, no. 1, 2019, doi: 10.1088/1757-899X/560/1/012114.
- [7] A. T. Malov, N. P. Rjashencev, A. P. Malahov, A. N. Antonov, and A. V. Nosovec, *Electromagnetic hammer*. Moscow: Nauka Publisher, 1979.
- [8] L. A. Neyman, N. I. Schurov, and E. G. Langeman, "New linear synchronous cycle electromagnetic machines with inertial reverse," *Proceedings - 2016 11th International Forum on Strategic Technology, IFOST 2016*, pp. 44–47, 2017, doi: 10.1109/IFOST.2016.7884290.
- [9] V. I. Moshkin, D. N. Shestakov, and G. G. Ugarov, "Energy Modes of the Pulse Linear Electromagnetic Motor with Effective Transformation of Magnetic Energy," *2018 International Multi-Conference on Industrial Engineering and Modern Technologies, FarEastCon 2018*, 2018, doi: 10.1109/FarEastCon.2018.8602832.
- [10] T. Wu, K. Fu, J. Zhu, and G. Lei, "The influence analysis of thrust and gap magnetic field of a down-to-hole tubular permanent magnet linear hammer due to high temperature in deep hole," *2017 20th International Conference on Electrical Machines and Systems, ICEMS 2017*, 2017, doi: 10.1109/ICEMS.2017.8056381.
- [11] J. Hong, S. Wang, Y. Sun, and H. Cao, "A method of modal parameter estimation based on electromagnetic vibration exciter," *2019 IEEE International Electric Machines and Drives Conference, IEMDC 2019*, pp. 1126–1129, 2019, doi: 10.1109/IEMDC.2019.8785228.
- [12] K. Hirata, T. Tanibe, and T. Ota, "Impact torque analysis of new electromagnetic impact mechanism employing 3-D finite element method," *Digests of the 2010 14th Biennial IEEE Conference on Electromagnetic Field Computation, CEFC 2010*, 2010, doi: 10.1109/CEFC.2010.5481215.
- [13] L. Hu, K. Yang, C. Suo, Y. Ding, and W. Yu, "Analysis of Radial Electromagnetic Force in Permanent Magnet Machine with Manufacturing Tolerance," *ICEMS 2018 - 2018 21st International Conference on Electrical Machines and Systems*, pp. 256–260, 2018, doi: 10.23919/ICEMS.2018.8549530.
- [14] L. A. Neyman, V. Y. Neyman, and K. A. Obukhov, "New method of the synchronous vibratory electromagnetic machine mechatronic module control," *International Conference of Young Specialists on Micro/Nanotechnologies and Electron Devices, EDM*, pp. 516–519, 2017, doi: 10.1109/EDM.2017.7981808.
- [15] F. Sun, X. Li, T. Jiang, and W. Zhang, "A Multi-axis vibration fixture based on electromagnetic shaker," *Proceedings of 2009 8th International Conference on Reliability, Maintainability and Safety, ICRMS 2009*, pp. 1183–1186, 2009, doi: 10.1109/ICRMS.2009.5270071.
- [16] L. A. Neyman, V. Y. Neyman, and A. V. Markov, "The processes of energy transformation in a two-coil synchronous electromagnetic shock machine," *International Conference of Young Specialists on Micro/Nanotechnologies and Electron Devices, EDM*, vol. 2018-July, pp. 767–770, 2018, doi: 10.1109/EDM.2018.8434926.
- [17] S. Zhang, L. Norum, R. Nilssen, and R. D. Lorenz, "Down-The-Hole hammer drilling system driven by a tubular reciprocating translational motion permanent magnet synchronous motor," *IEEE International Symposium on Industrial Electronics*, pp. 647–651, 2012, doi: 10.1109/ISIE.2012.6237165.




- [18] L. A. Neyman, V. Y. Neyman, and A. S. Shabanov, "Analysis of impact interaction of forces impulses in an electromechanical vibratory system with electromagnetic excitation," *International Conference of Young Specialists on Micro/Nanotechnologies and Electron Devices, EDM*, vol. 2018-July, pp. 763–766, 2018, doi: 10.1109/EDM.2018.8434984.
- [19] J. M. Zhang, F. Zhao, W. Wang, X. B. Ze, and D. N. Su, "Dynamic analysis of tip set extra hard load of vertical shaft impact crusher," *2009 International Conference on Measuring Technology and Mechatronics Automation, ICMTMA 2009*, vol. 3, pp. 71–74, 2009, doi: 10.1109/ICMTMA.2009.301.
- [20] G. Y. Lu, L. Zhifang, Z. Junhan, and S. Y. Zhang, "Measuring of impact force and the crush distance of the cylindrical shell impacted by MASS," *2009 International Conference on Measuring Technology and Mechatronics Automation, ICMTMA 2009*, vol. 1, pp. 241–243, 2009, doi: 10.1109/ICMTMA.2009.208.
- [21] Y. Li, H. Shan, and S. Huang, "Study on failure evolution process of fractured rock specimen under axial force," *Proceedings - 10th International Conference on Measuring Technology and Mechatronics Automation, ICMTMA 2018*, vol. 2018-January, pp. 387–390, 2018, doi: 10.1109/ICMTMA.2018.00100.
- [22] S. Takagawa, "A study on high frequency hammering system and its impact loads," *MTS/IEEE Seattle, OCEANS 2010*, 2010, doi: 10.1109/OCEANS.2010.5664398.
- [23] H. Liu, X. Zhang, and A. Luo, "Expansion tubes as impact energy absorbers: Experimental investigations and numerical simulations," *2017 IEEE International Conference on Mechatronics and Automation, ICMA 2017*, pp. 1366–1371, 2017, doi: 10.1109/ICMA.2017.8016016.
- [24] H. Chang, W. Zhou, Y. Hong, and J. Ye, "Output Force Characterization of the Electromagnetic Calibration Device for Low Thrust Measurement," *IEEE Transactions on Instrumentation and Measurement*, vol. 70, 2021, doi: 10.1109/TIM.2021.3063197.
- [25] Z. Han, J. Xu, W. Rui, L. Wang, and G. Li, "Analysis of Electromagnetic Force of Linear Induction Motor with Segmented Power Supply for Electromagnetic Emission," *2020 Asia Energy and Electrical Engineering Symposium, AEEES 2020*, pp. 91–95, 2020, doi: 10.1109/AEEES48850.2020.9121442.

BIOGRAPHIES OF AUTHORS



Ayman Y. Al-Rawashdeh    was born on 01 January 1970 in Jordan. He obtained his Diploma degree in 1995 and PhD degree in 2008 in the field of Mechatronics Engineering. Currently, Dr. Al-Rawashdeh is an Associate Professor at the Department of Electrical Engineering, Faculty of Engineering Technology, Al-Balqa Applied University, Jordan. His main research interests include renewable energy, drive system analysis and simulations. He can be contacted at email: dr.ayman.rawashdeh@bau.edu.jo.



Vlademer E. Pavlov    is an Associate Professor in the Department of Mechatronics Engineering, Irkutsk National Research Technical University, Russia. Dr. Pavlov was born on 1952. His main research interests include power converter technology, expert systems for setting up electrical equipment, automation and process control. He has published more than 140 journal papers in the fields of electric drives and its applications. He can be contacted at email: pvew52@mail.ru.